



ELSEVIER

Nuclear Instruments and Methods in Physics Research A 426 (1999) 583-598

NUCLEAR  
INSTRUMENTS  
& METHODS  
IN PHYSICS  
RESEARCH  
Section A

# Structure function measurements and kinematic reconstruction at HERA

Ursula Bassler, Gregorio Bernardi\*

Laboratoire de Physique Nucléaire et des Hautes Energies, Université Paris 6-7, 4 Place Jussieu, 75252 Paris Cedex 05, France

Received 2 November 1998

## Abstract

The procedure used for structure function measurements at HERA is briefly described and related to the properties of kinematic reconstruction. The reconstruction methods of the inclusive deep inelastic scattering variables are reviewed and their sensitivity to the energy and angle miscalibrations are discussed in detail. New prescriptions are introduced and related to the standard methods in order to optimize the  $F_2$  structure function measurement over the widest kinematic range, both in the low  $x$ , low  $Q^2$  and in the high  $x$ , high  $Q^2$  regions. The prospects for the future high  $Q^2$  studies are briefly discussed. © 1999 Elsevier Science B.V. All rights reserved.

**Keywords:** Deep inelastic scattering; HERA; Structure functions; Kinematic reconstruction; Systematic effects

## 1. Introduction

The measurement of the structure functions of the nucleon is a major tool for the study of the strong interaction and the behavior of the parton densities in the hadrons. To reveal possible non-standard small deviations from their well-established behaviour described by the DGLAP [1-3] evolution equations, such as BFKL effects at low  $x$  or the presence of intrinsic charm in the proton at high  $x$  to name just two of them, requires a precise reconstruction of the deep-inelastic scattering (DIS) kinematics over the widest possible kinematic

range. With the advent of the HERA electron-proton collider, this reconstruction no longer needs to rely on the scattered lepton only, since the most important part of the hadronic system is visible in the almost hermetic H1 and ZEUS detectors. This redundancy allows for an experimental control of the systematic errors and of the radiative corrections to the structure function measurement if it is based on several independent methods to determine the usual DIS kinematic variables  $x, y, Q^2$ :

$$x = \frac{Q^2}{2Pq}, \quad y = \frac{Pq}{Pk}$$

$$Q^2 = -(k - k')^2 = -q^2 = xys \quad (1)$$

with  $s$  being the ep center of mass energy squared,  $P, k$  the 4-vectors of the incident proton and lepton, and  $k'$  of the scattered lepton. Since many different

\* Corresponding author. Tel.: +1-33-1-44-27-47-94; fax: +1-33-1-44-27-46-38.

E-mail address: gregorio@mail.desy.de (G. Bernardi)

reconstruction methods have already been used at HERA, it is a natural objective to optimize this reconstruction, and to try to find the “best” method, or at least to justify the use of a given method instead of a kinematic fitting algorithm for instance. In this report we briefly sketch in Section 2 the procedure used so far to measure  $F_2$  at HERA, and relate it to the effects of kinematic reconstruction. In Section 3 we review the methods of kinematic reconstruction used at HERA, and we classify them on the basis of their properties. In Section 4 we discuss possible improvements of these reconstruction methods, in particular those related to the study of low  $x$  physics. In Section 5 we study the effect of the hadronic final state and scattered electron reconstruction errors on the kinematic methods in order to understand the choices made in this field by the two HERA collaborations. In Section 6, the high  $Q^2$  case is treated in more detail due to its future importance and also since there are new possibilities in this kinematic regime. In conclusion, we briefly provide some prospects on the influence of these technical matters on the structure function measurement program of the next decade.

## 2. Structure function measurements

The cross-section for the DIS reaction  $e^+ + p \rightarrow e^+ + X$  with unpolarized beams is

$$\frac{d^2\sigma}{dx dQ^2} = \frac{2\pi\alpha^2}{xQ^4} [Y_+ F_2(x, Q^2) - y^2 F_L(x, Q^2) - Y_- xF_3(x, Q^2)] (1 + \delta_r) \quad (2)$$

In this equation  $\alpha$  is the electromagnetic coupling,  $F_2$  is the generalized structure function which reflects both photon and  $Z^0$  exchange,  $F_L$  is the longitudinal structure function,  $xF_3$  is a structure function arising only from the  $Z^0$  exchange,  $\delta_r$  is the electroweak radiative correction. The helicity dependence of electroweak interactions, is contained in the functions  $Y_{\pm} = 1 \pm (1 - y)^2$ .

At HERA, these three structure functions of the proton can be measured, in particular  $F_2$  which has already been measured over several orders of magnitude in  $x$  and  $Q^2$  with a precision of about 5%.

Although apparently only one observable ( $d^2\sigma/dx dQ^2$ ) is related to the three structure functions, the problem can be solved because in some kinematic region only one of them has a relevant contribution and/or because the beam conditions (energy, lepton sign) can be changed, hence changing the coefficient in front of each of them, for a given  $d^2\sigma/dx dQ^2$ . In the following, we will not study the procedure to derive them from the cross-section measurement (which are described in Ref. [4] for instance), but concentrate on the determination of  $d^2\sigma/dx dQ^2$ .

Generally, the value of  $d^2\sigma/dx dQ^2$  at the point  $(x_0, Q_0^2)$  is experimentally determined by the number  $N_{\Delta}^D$  (“D” stands for Data) of DIS events observed in an  $(x, Q^2)$  bin  $\Delta$  centered around  $(x_0, Q_0^2)$ , normalized to the integrated luminosity  $L^D$  accumulated during the data taking and corrected by an acceptance factor  $T_{\Delta}^D$  which depends on the event selection cuts and on the detector response:

$$\frac{d^2\sigma}{dx dQ^2} = \frac{C_{\Delta} N_{\Delta}^D}{L^D T_{\Delta}^D} \quad (3)$$

$C_{\Delta}$  is a numerical factor which takes into account the surface of the bin. Actually, resolution effects cause migration of events from one bin to other bins, so the previous relation should be treated in fact as a matrix relation, with the cross-section being related to all bins via the inverse of a matrix  $T(ij)$ , in which every matrix element  $(ij)$  gives the probability that an event originating from the bin  $i$  is reconstructed in a bin  $j$ . Thus the double differential cross-section measured at the center of the bin  $(i)$  is

$$\frac{d^2\sigma}{dx dQ^2} = \frac{C_{\Delta}}{L^D} \sum_j N_j^D T^{-1}(ij) \quad (4)$$

The matrix  $T$  can be obtained by simulating a large sample of DIS events, provided the simulation is able to reproduce the detector effects. However to solve Eq. (4) one needs to invert this matrix. This is a non-trivial task due in particular to numerical instabilities [5–7], which has not been done yet for the published HERA structure function measurements. Instead, an iterative procedure is used to solve Eq. (3). Obviously, if the structure function used in the simulation is equal to the one to be

measured  
for simul

$$\frac{d^2\sigma}{dx dQ^2} =$$

This equ  
simulatio  
metrizati  
the para  
structure  
ation. In  
within 1  
discussio  
measured  
by value  
them in  
their rela  
will now

We dis  
one  $(\Delta, t)$   
defined a  
on the r  
the effect  
ber of e  
events be  
posed to  
but can b  
events in  
clearly b  
deduce fi  
[9,10]

$$T_{\Delta} = \frac{N_{\Delta}^c}{N_{\Delta}^e}$$

$$A_{\Delta} = \frac{N_{\Delta}^c}{N_{\Delta}^e}$$

The first  
the cuts i  
defined a  
since onl  
struction  
are choo  
discuss h  
might oc  
and on th  
the smear  
ations (u)

measured, and assuming that  $T_{\Delta}^D = T_{\Delta}^S$  ("S" stands for simulation), we have

$$\frac{d^2\sigma}{dx dQ^2} = \frac{N_{\Delta}^D L^S}{L^D N_{\Delta}^S} \frac{d^2\sigma^S}{dx dQ^2} \quad (5)$$

This equation is solved iteratively, starting the simulation from a "guessed" structure function parametrization, and replacing it at each iteration by the parametrization obtained from a fit to the structure function "measured" at the previous iteration. In three or four iterations the result is stable within 1% or less (see Ref. [8] for a more detailed discussion) in the measureable regions. These measureable regions are empirically characterized by values of  $T_{\Delta}$  close to unity. In order to define them in a more rigorous way and to understand their relation to the kinematic reconstruction, we will now study the  $T_{\Delta}$  factors.

We distinguish two ways of defining the bin  $\Delta$ : one  $(\Delta, t)$  based on the "true" kinematic variables, defined at the hadronic vertex; the other  $(\Delta, r)$  based on the reconstructed variables. We also consider the effect of the "event selection cuts" on the number of events ( $N_{\Delta}^c$ ) compared to the number of events before the cuts ( $N_{\Delta}$ ). These "cuts" are imposed to improve the precision of the measurement, but can have an influence on the distribution of the events in the kinematic plane, so the two cases must clearly be separated. With these definitions, we deduce from Eq. (3) that  $T_{\Delta}$  can be expressed as [9,10]

$$T_{\Delta} = \frac{N_{\Delta, r}^c}{N_{\Delta, t}^c} = \varepsilon_{\Delta, t} \cdot A_{\Delta} \quad \text{with } \varepsilon_{\Delta, t} \equiv \frac{N_{\Delta, t}^c}{N_{\Delta, t}} \quad \text{and} \quad A_{\Delta} \equiv \frac{N_{\Delta, r}^c}{N_{\Delta, t}^c} \quad (6)$$

The first term ( $\varepsilon_{\Delta, t}$ ) characterizes the "efficiency" of the cuts in the bin  $\Delta$ , while the second one can be defined as the "smearing acceptance" of the bin  $\Delta$ , since only the smearing of the kinematic reconstruction is involved in its variations. Since the cuts are chosen to have a high efficiency, we will not discuss here the difference at the percent level which might occur between  $\varepsilon_{\Delta}$  as determined on the data and on the simulation, but focus on the behavior of the smearing acceptance, which can have large variations (up to hundreds of percents) across the kin-

ematic plane, hence determining the measureable regions. The smearing acceptance variations are better studied considering the  $(\Delta, i)$  subset which contains the events belonging to  $(\Delta, i)$  and  $(\Delta, r)$ . Then  $A_{\Delta}$  can be rewritten as

$$A_{\Delta} = \frac{S_{\Delta}}{P_{\Delta}} \quad \text{with } S_{\Delta} \equiv \frac{N_{\Delta, i}^c}{N_{\Delta, t}^c} \quad \text{and} \quad P_{\Delta} \equiv \frac{N_{\Delta, i}^c}{N_{\Delta, r}^c}, \quad N_{\Delta, i} \equiv N_{\Delta, t \cap \Delta, r} \quad (7)$$

$S_{\Delta}$  and  $P_{\Delta}$  are referred as the stability and the purity of the bin  $\Delta$ , since they characterize respectively:

- The proportion of genuine events of a bin, which are reconstructed in the same bin.  $S_{\Delta}$  characterizes the number of events which migrate *outside* of the bin  $\Delta$ .
- The ratio of genuine events of a bin reconstructed in the same bin divided by the total number of events reconstructed in that bin. This last number is influenced by the number of events originating from other bins which migrate *into*  $\Delta$ .

The obvious goal is to maintain a stability and a purity as close to unity as possible, hence  $A_{\Delta}$  will also be close to 1. However  $A_{\Delta}$  can be close to unity even for a low stability bin, if its purity roughly matches its stability. In order to ensure a reliable measurement of the cross-section, we will thus enforce conditions on  $S_{\Delta}$  and  $P_{\Delta}$  separately, rather than only on their ratio. To make a concrete example let us examine the three standard reconstruction methods used for DIS neutral currents at HERA, in the  $(x, Q^2)$  binning used by the H1 collaboration, i.e. 8 (5) bins per order of magnitude in  $Q^2$  ( $x$ ) [11]. The smearing acceptance, stability and purity for the H1 detector are shown in Fig. 1 for the electron, Double-angle [12,13] and  $\Sigma$  [14] methods, in  $x$  bins, at  $Q^2 = 20 \text{ GeV}^2$ . As mentioned, the acceptance can be equal to unity, while the stability and the purity are low ( $\sim 25\%$ ), like for instance at the lowest  $x$  point in the DA method. Conversely, by requiring a "reasonably" high stability and purity (we will use throughout this paper a minimum of 30%, as the H1 collaboration did for this binning [11]), we ensure an acceptance close to unity.

We observe in Fig. 1 that the stability has a more regular behaviour than the purity or the

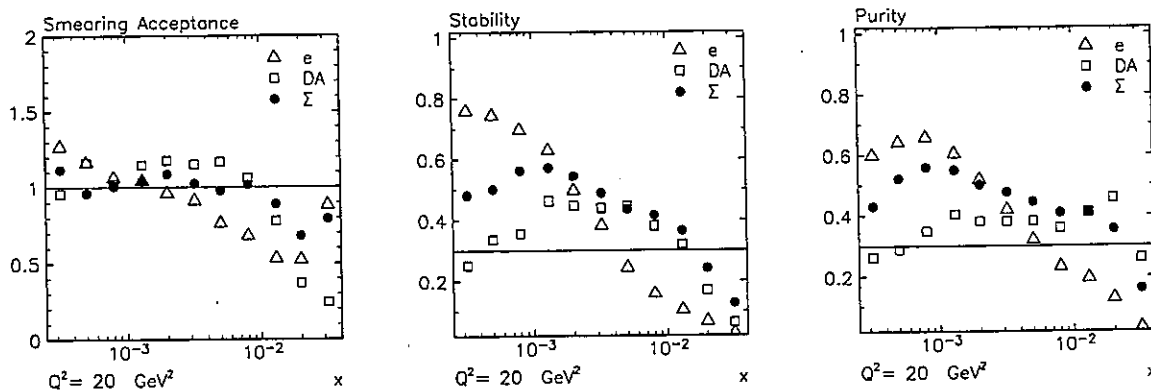


Fig. 1. Smearing acceptance, stability and purity at  $Q^2 = 20 \text{ GeV}^2$  for the three kinematic reconstruction methods: e (open triangles), DA (open squares),  $\Sigma$  (closed circles).

acceptance, since it reflects only the combination of the resolutions in  $x$  and  $Q^2$  in a given bin. The stability can be increased by enlarging the size of the bin. Although the stability and purity are related quantities (they share the same numerator), the purity is more irregular because it is influenced by events coming from other bins, which may be populated in a different way, and have different resolutions in the kinematic variables. Like the stability, the purity can also be increased by enlarging the bin size; however the migrations inside the bin depend on several factors (resolutions in different bins, population of different bins, structure function values in regions which are not "measurable", radiative effects), rendering the control of the purity more delicate than the stability. Thus, in the following, when comparing different methods, we will make the comparison on their purity, but only in the bins having a minimum stability (chosen to be 30%).

**3. Kinematic reconstruction methods at HERA**

In the naive quark-parton model (QPM), the lepton scatters elastically with a quark of the proton, and the two body final state is completely constrained using two variables, if we know the initial energies labeled  $E_0$  and  $P_0$  of the electron and proton. Similarly, the DIS variables can be determined using two independent variables, which

can be the energy ( $E$ ) of the scattered electron, its polar angle<sup>1</sup> ( $\theta$ ) or independent quantities reconstructed out of the hadronic final state particles. For instance  $\Sigma$ , obtained as the sum of the scalar quantities  $E_h - p_{z,h}$  of each particle (assumed to be massless) belonging to the hadronic final state,  $p_{T,h}$  as its total transverse momentum or the inclusive angle  $\gamma$  of the hadronic system<sup>2</sup> which corresponds to the angle of the scattered quark in the QPM:

$$\Sigma = \sum_h (E_h - p_{z,h}),$$

$$p_{T,h} = \sqrt{\left(\sum_h p_{x,h}\right)^2 + \left(\sum_h p_{y,h}\right)^2},$$

$$\tan\left(\frac{\gamma}{2}\right) = \frac{\Sigma}{p_{T,h}}. \tag{8}$$

$E_h, p_{x,h}, p_{y,h}, p_{z,h}$  are the four-momentum vector components of each hadronic final state particle.  $\Sigma$  is by construction minimally affected by the losses in the forward direction due to the beam pipe hole in which the target jet and the initial state gluon

<sup>1</sup>The positive  $z$ -axis is defined at HERA as the incident proton beam direction.

<sup>2</sup>We can define the similar quantities for the scattered electron:  $\Sigma_e = E(1 - \cos \theta), p_{T,e} = E \sin \theta$ , i.e.  $\tan(\theta/2) = \Sigma_e/p_{T,e}$ .

radiation tend to disappear spatial dimensions, and in losses. Thus to improve resolution we should avoid using  $\gamma$  instead, which carries better measured since in uncertainties cancel to first order the losses in the forward direction. Thus the optimal four "variables" to characterize deep inelastic scattering are  $[E, \theta, \Sigma, \gamma]$ .

Using these four independent basic methods which measure at a time, and which are a sensible kinematic reconstruction

- The electron only method and  $\theta$ .
- The double-angle method  $\gamma$  [12,13].
- The hadrons only method  $\Sigma$  [15]

In the following, all methods using some information about the final state will be called "hadronic" (speaking there is one method (a complete set of variables) in appendix). The hadronic method in the following since compared to the other events.

More than two variables are needed to describe the kinematics if the initial state is not a photon which is the case when a photon before the hadronic system is often undetected since the incident electron beam escape inside the beam pipe. For instance,  $y_h = \Sigma / (\Sigma + \Sigma_e)$  to take into account the energy due to the escape of the electron. An important characteristic becomes the dominant and thus experimental uncertainties tend to cancel in the denominator. In the constructed, like  $y_{\Sigma}$

radiation tend to disappear.  $p_{T,h}$  covers the other spatial dimensions, and is more sensitive to forward losses. Thus to improve the kinematic reconstruction we should avoid using  $p_{T,h}$  directly. We can use  $\gamma$  instead, which carries the  $p_{T,h}$  information and is better measured since in the ratio  $\Sigma/p_{T,h}$  the energy uncertainties cancel to first order and the effect of the losses in the forward beam pipe is diminished. Thus the optimal four "detector oriented" variables to characterize deep inelastic scattering at HERA are  $[E, \theta, \Sigma, \gamma]$ .

Using these four input variables, there are three basic methods which make use of only two of them at a time, and which are precise enough to allow sensible kinematic reconstruction, namely:

- The electron only method (e) which uses  $E$  and  $\theta$ .
- The double-angle method (DA) which uses  $\theta$  and  $\gamma$  [12,13].
- The hadrons only method (h) which uses  $\Sigma$  and  $\gamma$  [15]

In the following, all methods (for instance the DA) using some information from the hadronic final state will be called "hadronic", although strictly speaking there is only one inclusive hadronic method (a complete set of formulae is given in the appendix). The h method will not be discussed in the following since it is not precise enough compared to the others, for neutral current DIS events.

More than two variables are needed to determine the kinematics if the incident energy is unknown, which is the case when the incident electron emits a photon before the hard collision. This photon is often undetected since it is emitted colinearly with the incident electron beam direction, and can thus escape inside the beam pipe. In this case three variables are needed to reconstruct the kinematics. For instance,  $y_h = \Sigma/2E_0$  can be replaced by  $y_\Sigma \equiv \Sigma/(\Sigma + \Sigma_e)$  to take into account the missing energy due to the escaping photon. A further important characteristic of  $y_\Sigma$  is that at high  $y$ ,  $\Sigma$  becomes the dominant term in the denominator and thus experimental errors on the  $\Sigma$  measurement tend to cancel between numerator and denominator. In the  $\Sigma$  method [14],  $Q_\Sigma^2$  is constructed, like  $y_\Sigma$  to be independent of QED

initial state radiation (ISR) and to be optimal in terms of resolution; thus  $p_{T,e}$  is used instead of  $p_{T,h}$ :

$$Q_\Sigma^2 \equiv p_{T,e}^2/(1 - y_\Sigma) \quad x_\Sigma \equiv Q_\Sigma^2/sy_\Sigma \quad (9)$$

Insensitivity to ISR on  $x_\Sigma$  is achieved simply by replacing  $s$  by  $2P_0(\Sigma + \Sigma_e)$ , thereby obtaining the  $I\Sigma$  method which is based on  $(E, \theta, \Sigma)$ . The DA method was also rendered ISR independent by using  $E$  to reconstruct the initial electron beam energy. The IDA method [12,13] obtained in this way is thus based on  $(E, \theta, \gamma)$ . The complete formulae and the comparison of these two methods can be found in Ref. [14]. They will not be considered in the following, since the gain obtained by the complete independence to ISR is not sufficient to compensate the loss of precision induced by the reconstruction of the incident electron energy.

Fig. 2 shows the purity of the e, DA and  $\Sigma$  methods as a function of  $x$  in bins of  $Q^2$ . The properties of the three standard methods to reconstruct the kinematics of neutral current DIS events at HERA are clearly visible: high precision of the e method at high  $y$  with a severe degradation at low  $y$ , good precision for the  $\Sigma$  method in the complete kinematic range, high precision of the DA method at medium ( $\sim 10^2 \text{ GeV}^2$ ) and high  $Q^2$  ( $\sim 10^4 \text{ GeV}^2$ ) with a severe degradation at low  $Q^2$  ( $\sim 1 \text{ GeV}^2$ ).

The "hadronic" methods have already been shown to display at low  $x$  and low  $Q^2$  a rather imprecise reconstruction of  $Q^2$ . A simple solution to this problem is to use  $Q_e^2$  and to obtain, via  $Q^2 = xys$ , either  $x$  from a hadronic  $y$  or  $y$  from a hadronic  $x$ . For instance we have the mixed method [16] ( $x_m$  is obtained from  $y_h$  and  $Q_e^2$ ) which has a good precision at low  $y$  [17,18]. The precision at high  $y$  can be improved by using the mixed  $\Sigma$  ( $m\Sigma$ ;  $y_{m\Sigma} \equiv y_\Sigma$  and  $Q_{m\Sigma}^2 \equiv Q_e^2$ ), or better the e $\Sigma$  method ( $x_{e\Sigma} \equiv x_\Sigma$  and  $Q_{e\Sigma}^2 \equiv Q_e^2$ ) as was shown in Figs. 2 and 3 of Ref. [14].

Another approach to combining two methods which have complementary properties has been tried by the H1 collaboration in the analysis of the diffractive structure function [19]. Since  $Q^2 = 4E_0^2(1 - y)/\tan^2(\theta/2)$  both in the e and DA methods, an "average" method (labeled here ADA) has been introduced, in which  $y_{ADA}$  is obtained by

e  
DA  
 $\Sigma$   
  
x  
angles)  
  
on, its  
recon-  
structs.  
scalar  
to be  
state,  
clus-  
corre-  
n the  
  
(8)  
  
ector  
cle.  $\Sigma$   
osses  
hole  
gluon  
  
cident  
1 elec-

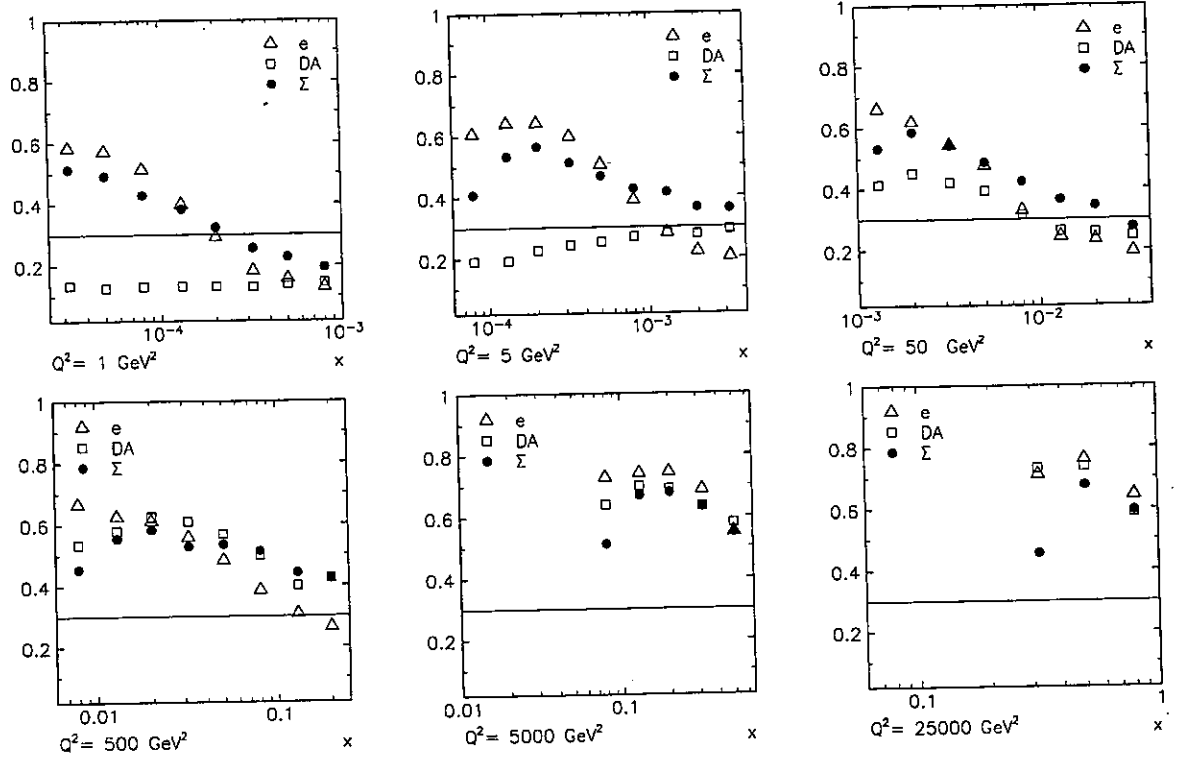


Fig. 2. Purity at  $Q^2 = 1, 5, 50, 500, 5000$  and  $25000 \text{ GeV}^2$  for the three kinematic reconstruction methods: e (open triangles), DA (open squares),  $\Sigma$  (closed circles).

weighting  $y_e$  and  $y_{DA}$  by  $y$  and  $(1 - y)$  respectively,

$$y_{ADA} \equiv y_e^2 + y_{DA}(1 - y_{DA}),$$

$$Q_{ADA}^2 \equiv \frac{4E_0^2(1 - y_{ADA})}{\tan^2(\theta/2)}. \quad (10)$$

On the non-diffractive DIS events a better complementarity is actually achieved in the  $A\Sigma$  method by “averaging” the e and the  $\Sigma$  methods [20]. However neither the  $A\Sigma$  nor the ADA method bring an improvement compared to the simpler  $e\Sigma$  method as can be seen in Fig. 3: the  $A\Sigma$  method is giving similar performances to the  $e\Sigma$  one except at low  $x$  where it is slightly less precise, while the ADA method is better at high  $x$  and high  $Q^2$ , but weaker elsewhere, in particular at low  $Q^2$ .

Before ordering these methods to underline their relations, let us introduce another method derived from the DA method, which will be

useful later, for the understanding of more complicated methods and for the study of error propagation. Following the logic used for the  $\Sigma$  method, the inclusive hadronic angle  $\gamma$  can be replaced by  $\gamma_\Sigma$  defined by  $\tan(\gamma_\Sigma/2) = \Sigma/p_{T,e}$  since transverse momentum conservation implies  $p_{T,h} = p_{T,e}$  even in the case of collinear ISR. This replacement improves the precision on the hadronic angle but has the obvious drawback of introducing a sensitivity to the electron energy reconstruction errors, which is absent in the DA method. This  $D\Sigma$  method defined using  $\gamma_\Sigma$  instead of  $\gamma$  in the DA formulae, gives

$$y_{D\Sigma} = \frac{\tan(\gamma_\Sigma/2)}{\tan(\gamma_\Sigma/2) + \tan(\theta/2)} = \frac{\Sigma/p_{T,e}}{\Sigma/p_{T,e} + \Sigma_e/p_{T,e}} = y_\Sigma. \quad (11)$$

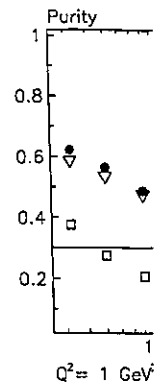


Fig. 3. Purity at  $Q^2 = 1 \text{ GeV}^2$  (closed circles).

The  $Q_{D\Sigma}^2$  and their  $\Sigma$  counts will see in the electron miscal

In Fig. 4 the  $x(x_{rec})$  divided lent distributio  $\Sigma$ ,  $D\Sigma$  method all the figures a deep-inelasti H1 detector (1: All known effe the physics poi radiation) are i been shown to data in the cor uncertainty o angle and on t 1%, 1 mrad at a cut at  $Q^2 \geq$  ponds at HEL highest precis at low  $x$  and visible. Only though lower,

<sup>3</sup> At low  $y$ , si results in terms strongly degrad plots of the pur almost identical

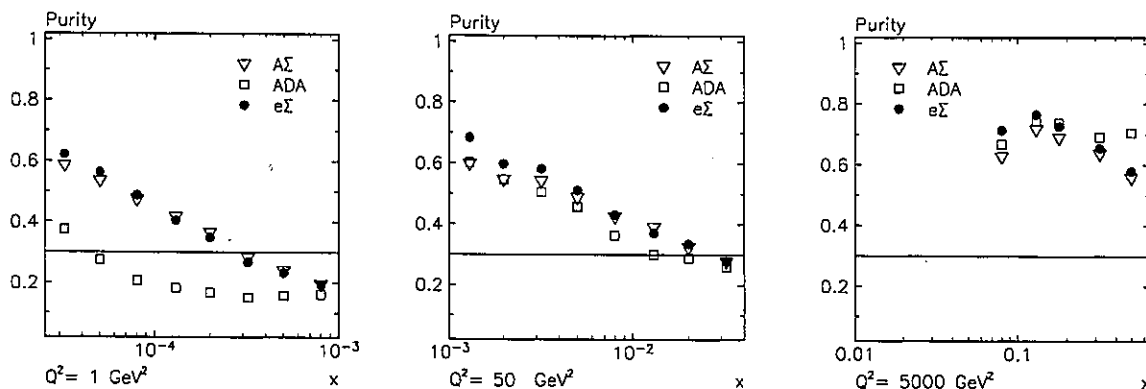


Fig. 3. Purity at  $Q^2 = 1, 50$  and  $5000 \text{ GeV}^2$  for the three kinematic reconstruction methods: AΣ (open triangles), ADA (open squares), eΣ (closed circles).

The  $Q_{D\Sigma}^2$  and  $x_{D\Sigma}$  are nevertheless different from their  $\Sigma$  counterparts (although  $x_{D\Sigma} = x_m$ ) and we will see in the Section 5 how the hadronic and electron miscalibrations affect them.

In Fig. 4 the distribution of the reconstructed  $x$  ( $x_{\text{rec}}$ ) divided by the true  $x$  ( $x_{\text{gen}}$ ) and the equivalent distribution for  $Q^2$  are compared for the e, DA,  $\Sigma$ , DΣ methods at high  $y$  (0.3–0.7).<sup>3</sup> This figure, as all the figures in this paper, is obtained from a deep-inelastic sample simulated in detail in the H1 detector (1995 set-up) as described in Ref. [21]. All known effects both from the detector and from the physics point of view (structure functions, QED radiation) are included in the simulation, which has been shown to give a good description of the H1 data in the complete kinematic range [21–23]. The uncertainty on the electron energy, on the polar angle and on the hadronic energy scale are typically 1%, 1 mrad and 4% respectively. For Figs. 4 and 5, a cut at  $Q^2 \geq 7 \text{ GeV}^2$  has been made, which corresponds at HERA to the region measured with the highest precision. In Fig. 4 the excellent resolution at low  $x$  and low  $Q^2$  of the e method is clearly visible. Only the  $\Sigma$  method has a comparable, although lower, resolution in  $x$ . In  $Q^2$  the weakness of

all these hadronic methods is visible. The DΣ method is more precise than the DA one at low  $Q^2$ , as expected from the way it is constructed. Unfortunately the e method is not precise at low  $y$  (as can be seen in Fig. 2), so either the structure function measurement is done using different methods in different regions of the kinematic plane, or a precise method over the complete kinematic plane is found. Both these approaches have already been used at HERA, but for the more precise future measurements it is mandatory to focus on the second case and to optimize the reconstruction method to be used.

To conclude this section, the hadronic methods are ordered in Table 1: each column represents the type of approach followed (sigma, double-angle, mixed), while each row represents a prescription to derive them: basic method, ISR independent, “optimized resolution”. The relations become clear and the effects coming from the type of reconstruction used can be disentangled, by comparing methods from the same row, from those due to the detector response which can be studied by comparing methods from the same column.

#### 4. Kinematic reconstruction improvements

The description of the methods given above suggests that it might be possible to further optimize the reconstruction precision. The most direct way would be to perform a fit of the kinematics using all

<sup>3</sup> At low  $y$ , since all hadronic methods give rather similar results in terms of resolution, (contrary to the e method which strongly degrades), the comparison is better made using the plots of the purity (Fig. 2). The purity of the DΣ method is almost identical to the  $\Sigma$  one at low  $y$  (not shown).

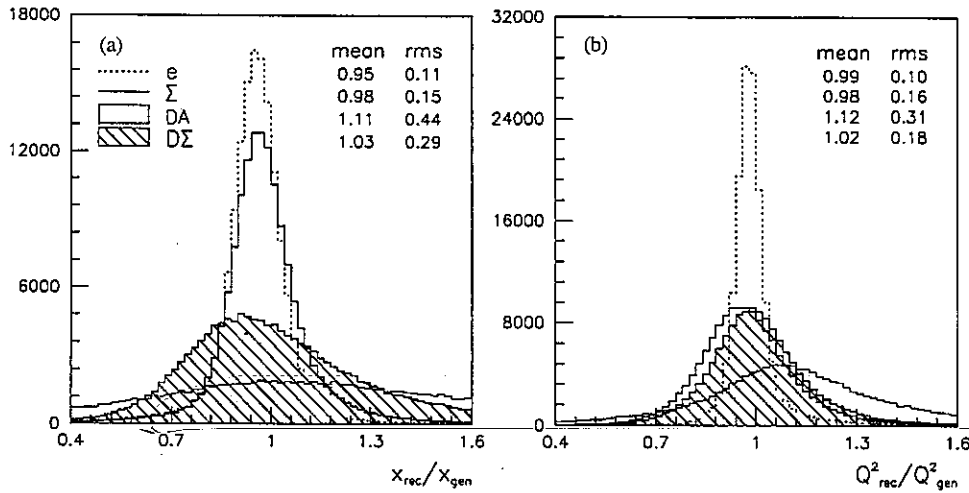


Fig. 4. Distribution of  $x_{rec}/x_{gen}$  (a) and  $Q^2_{rec}/Q^2_{gen}$  (b) for the e, DA,  $\Sigma$  and  $D\Sigma$  methods for  $Q^2 > 7 \text{ GeV}^2$  at high  $y$  ( $0.3 < y < 0.7$ ).

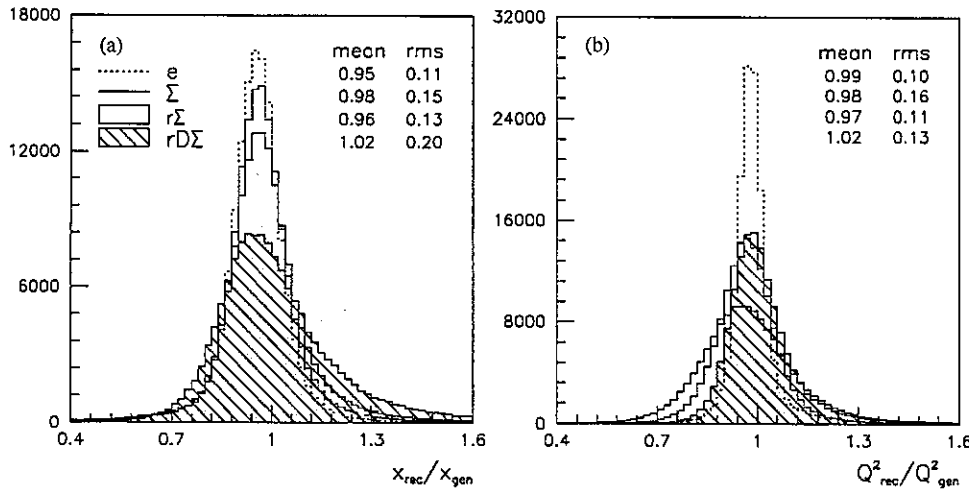


Fig. 5. Distribution of  $x_{method}/x_{gen}$  (a) and  $Q^2_{method}/Q^2_{gen}$  (b) for the e,  $\Sigma$ ,  $r\Sigma$  and  $rD\Sigma$  ( $\equiv$  PT) methods for  $Q^2 > 7 \text{ GeV}^2$  at high  $y$  ( $0.3 < y < 0.7$ ).

information available as described for instance in [24,25]. However the redundancy is not large, since  $p_{T,h}$  is not precise enough to be helpful in neutral current events, except at high  $Q^2$ . Furthermore, the method requires a good knowledge of the uncertainties of the measured variables over all the kinematic plane and the lack of statistics has prevented the production of a detailed enough map of all imperfections of the detectors. We will thus concentrate on the “analytic” improvement of the hadronic methods, in particular by “rescaling” the

hadronic energy:  $\Sigma$  may be rescaled to approach its true value using the formula  $\Sigma + \Sigma_e = 2E_0$ , if the error on  $\Sigma_e$  is assumed to be small compared to the  $\Sigma$  one.<sup>4</sup> But if  $\Sigma$  is expressed as  $2E_0 - \Sigma_e$  in the h or

<sup>4</sup>Indeed, the relative error on  $\Sigma$  increases when going to lower  $x$  and lower  $Q^2$  since the hadronic final state contains an increasing fraction of low energy particles which are measured less precisely and which may go undetected in the HERA detectors.

Table 1  
Classification of the hadronic energy methods. The Double-angle approach is also given. Note that the methods are defined in  $y$ . The methods described in Section 4

Basic method
ISR independent
Optimized method
Rescaled method

$\Sigma$  method, these methods are compared to the e method. An interesting comparison is made between the  $\Sigma$  and e method (corrected for the rescaling factor defined

$$r \equiv \frac{2E_0}{\Sigma + \Sigma_e}$$

as was already implicitly discussed previously.

$$y_\Sigma = ry_h, \quad y_{e\Sigma} = ry_e$$

An improvement of the method at low  $x$  is obtained by defining an  $r\Sigma$  method

$$y_{r\Sigma} \equiv \frac{r\Sigma}{r\Sigma + \Sigma_e} \quad (5)$$

The corresponding method is defined as  $\tan \gamma_{r\Sigma} = \Sigma_e / (r\Sigma + \Sigma_e)$ , a rescaled  $D\Sigma$  method is already derived in the HERA collaboration, and is compared to the e method. Similarly an  $re\Sigma$  method is defined as  $Q^2_{re\Sigma} = Q^2_e$ . With these definitions, the methods are compared in Table 1 with the “basic” methods. The  $x$  and  $Q^2$  in Fig. 5

<sup>5</sup>Actually, the “PT” method is defined using the hadronic final state using the definition of the method

Table 1

Classification of the hadronic methods. For the methods using the Double-angle approach, the corresponding hadronic angle is also given. Note that the  $m\Sigma$  method is ISR independent only in  $y$ . The methods displayed in the last row are discussed in Section 4

	Sigma	Double-angle	Mixed
Basic method	h	DA ( $y$ )	m
ISR independent	$I\Sigma$	IDA ( $y$ )	$m\Sigma$
Optimized method	$\Sigma$	D $\Sigma$ ( $y_\Sigma$ )	e $\Sigma$
Rescaled method	$r\Sigma$	PT ( $y_{r\Sigma}$ )	re $\Sigma$

$\Sigma$  method, these methods become identical to the e method. An intermediate solution between the  $\Sigma$  and e method can be obtained by using the rescaling factor defined as

$$r \equiv \frac{2E_0}{\Sigma + \Sigma_e} \quad (12)$$

as was already implicitly done in some of the previously discussed variables:

$$y_\Sigma = ry_h, \quad y_{e\Sigma} = ry_{e\Sigma}, \quad Q_\Sigma^2 = \frac{Q_e^2}{r}, \quad Q_{D\Sigma}^2 = Q_e^2 r. \quad (13)$$

An improvement on the  $\Sigma$  kinematic variables at low  $x$  is obtained by directly rescaling  $\Sigma$ , thereby defining an  $r\Sigma$  method:

$$y_{r\Sigma} \equiv \frac{r\Sigma}{r\Sigma + \Sigma_e}, \quad Q_{r\Sigma}^2 \equiv \frac{p_{T,e}^2}{1 - y_{r\Sigma}}. \quad (14)$$

The corresponding "rescaled" hadronic angle is defined as  $\tan \gamma_{r\Sigma} = r\Sigma/p_{T,e}$  and allows to define a rescaled D $\Sigma$  method ( $rD\Sigma$ ). This method was already derived in a different way by the ZEUS collaboration, and is called the "PT" method<sup>5</sup> [8]. Similarly an  $re\Sigma$  method is defined, using  $x_{r\Sigma}$  and  $Q_e^2$ . With these definitions we create the last row of Table 1 with the "rescaled" methods. These new methods are compared to the e and  $\Sigma$  methods in  $x$  and  $Q^2$  in Fig. 5 in the same  $Q^2, y$  intervals as

<sup>5</sup> Actually, the "PT" method includes also a calibration of the hadronic final state using  $p_{T,e}$ . Here we single out the analytic definition of the method.

those of Fig. 4. With the rescaling,  $x_{PT}$  ( $x_{r\Sigma}$ ) has indeed a better resolution than  $x_{D\Sigma}$  ( $x_\Sigma$ ). However,  $x_{PT}$  is still less precise for  $y$  values between 0.3 and 0.7. than the simple, non-rescaled,  $x_\Sigma$ , due to the propagation of the hadronic error in these two methods (cf. Section 5). The difference in  $x$  between the rescaled methods and the e method is now smaller, which is also true in  $Q^2$  where the rescaled methods ( $r\Sigma$  and PT) are similar and definitely better than the non-rescaled ones ( $\Sigma$  and D $\Sigma$ ). By using the  $Q_e^2$ , the  $re\Sigma$  combination allows a further improvement with respect to the two other rescaled methods or to the e $\Sigma$  method. The overall behaviour in the complete kinematic plane of one of the rescaled methods (the PT), compared to the e $\Sigma$  can be judged by their purity shown in Fig. 6. They both show a precise behaviour over the complete kinematic plane. The e $\Sigma$  method is more precise at low  $x$ , at high  $Q^2$ , and has a comparable or better purity than the e method (compare Figs. 2 and 6) even at low  $x$  and low  $Q^2$ .

Before examining in the next section the propagation of the errors on the kinematic variables, let us consider the other characteristic of the rescaling, i.e. the increased dependence on the electron variables, since the rescaling factor depends also on the reconstructed energy and angle of the scattered electron. We can indirectly demonstrate the increased dependence by applying a further rescaling, and obtain three new methods:  $r_2\Sigma, r_2D\Sigma$  and  $r_2e\Sigma$ . The  $r_2$  rescaling factor is obtained recursively (assuming  $r_0 = 1, r_1 = r$  and  $y_{r_0\Sigma} = y_\Sigma$ ) using the following formulae:

$$y_{r_n\Sigma} = \frac{y_{r_{n-1}\Sigma}}{y_{r_{n-1}\Sigma} + 1 - y_e} \quad \text{and} \quad r_n = \frac{2E_0}{r_{n-1}\Sigma + \Sigma_e}. \quad (15)$$

The resolution at high  $y$  improves at each rescaling and actually  $y_{r_n\Sigma} \rightarrow y_e$  when  $n \rightarrow \infty$ <sup>6</sup> implying that the three approaches ( $r_n\Sigma, r_nD\Sigma$  and  $r_ne\Sigma$ ) converge to the e method. This means that the gain in precision at high  $y$  is obtained at the expense of a loss of precision at low  $y$ . Furthermore the "hadronic"

<sup>6</sup> Since  $y_{r_n\Sigma}$  can be written as  $1/(1 + u + u^2 + \dots + u^{n-1} + u^n/y_\Sigma)$ , with  $u \equiv 1 - y_e$ .

